

# Liquid–Liquid Equilibrium Study in Ternary Castor Oil Biodiesel + Ethanol + Glycerol and Quaternary Castor Oil Biodiesel + Ethanol + Glycerol + NaOH Systems at (298.2 and 333.2) K

Alex Barreto Machado,<sup>†</sup> Yurany Camacho Ardila, Leonardo Hadlich de Oliveira, Martín Aznar, and Maria Regina Wolf Maciel\*

School of Chemical Engineering, University of Campinas, Av. Albert Einstein 500, CEP 13083-852, Campinas-SP, Brazil

 Supporting Information

**ABSTRACT:** In this work, ternary liquid–liquid equilibrium (LLE) data for the castor oil biodiesel (BIO–CO) + ethanol + glycerol and quaternary LLE data for biodiesel (BIO–CO) + ethanol + glycerol + NaOH systems at (298.2 and 333.2) K and atmospheric pressure ( $\approx 95$  kPa) were determined by gas chromatography. The influence of temperature and catalyst in the phase diagrams were studied. Ethanol partition coefficients and biodiesel selectivities were calculated. Results showed that ethanol distributed slightly more to the glycerol phase and that biodiesel solubilizes preferentially ethanol than glycerol. LLE experimental data were correlated with the NRTL model, presenting root-mean-square deviations  $< 1.3\%$ . Hand and Othmer–Tobias correlations were used to test the data quality, which presented  $R^2 > 0.98$  for all systems.

## INTRODUCTION

Biodiesel is a future prospective fuel and competes economically with petroleum diesel fuels. As an alternative for diesel engines, it has become important due to the future scarceness of petroleum reserves. As an environmental consequence, the emission of pollutants such as  $\text{SO}_x$ , CO, and  $\text{CO}_2$  will be reduced.<sup>1</sup> Biodiesel can be produced from biomass, such as oleaginous seeds and animal fats. It consists of a mixture of alkyl esters of fatty acids. Regarding soybean oil, it is a raw material widely available almost worldwide. Other oleaginous seeds are also used for biodiesel production like canola, cotton, sunflower, and castor. Methanol has been the most commonly used alcohol to perform transesterification reactions.<sup>2,3</sup> Ethanol has received some attention in the last decades, once it is derived from biomass<sup>4</sup> and so provides an alternative totally renewable biodiesel production.

Liquid–liquid equilibrium (LLE) data are essential for a proper understanding of the solvent extraction process. In the biodiesel industry this data can be used for understanding the process of purification and separation of biodiesel-rich phases from glycerol-rich phases. In the literature, liquid–liquid equilibrium data for biodiesel or fatty acid esters + alcohol + glycerol systems has been reported by Komers et al.,<sup>5</sup> Zhou et al.,<sup>6</sup> Negi et al.,<sup>7</sup> Andreatta et al.,<sup>8</sup> Liu et al.,<sup>9</sup> Tizvar et al.,<sup>10</sup> França et al.,<sup>11</sup> Barreau et al.,<sup>12</sup> and Follegatti-Romero et al.<sup>13</sup> LLE data involving systems with ethanolysis reagents were determined by Lanza et al.<sup>14</sup> Distribution of alcohol between two phases involving biodiesel systems were reported by Felice et al.<sup>15</sup>

In a previous paper,<sup>16</sup> the authors have studied the solubility curves in a system of soybean oil and castor oil biodiesel + ethanol + glycerol at different temperatures. However, tie lines or complete LLE data were not determined.

**Table 1. Properties of Other Chemicals used in This Work**

chemical	M		supplier
	$\text{g}\cdot\text{mol}^{-1}$	purity	
ethanol	46.07	$\geq 99.5$	Synth
glycerol	92.09	$\geq 99.5$	Synth
NaOH	40.00	$\geq 97.00$	Synth

This work is part of a larger study, in that LLE data for ternary and quaternary involving (soybean oil or castor oil biodiesel), ethanol, glycerol, water, NaOH systems at (298.2 and 333.2) K. Here, ternary liquid–liquid equilibrium (LLE) data for castor oil biodiesel (BIO–CO) + ethanol + glycerol and quaternary LLE data for biodiesel (BIO–CO) + ethanol + glycerol + NaOH systems at (298.2 and 333.2) K and atmospheric pressure ( $\approx 95$  kPa) were determined. Partition coefficients of ethanol were obtained, in order to investigate its behavior for future industrial biodiesel purification processes. The LLE data were correlated with the NRTL local composition model.

## EXPERIMENTAL SECTION

**Chemicals.** Castor oil biodiesel was produced, separated, purified, and characterized according to previous work,<sup>16</sup> which also describes its properties and characteristics. The synthesis procedure of this biodiesel does not affect considerably its composition, so, the mass fraction of ethyl esters present in the biodiesel used here is 0.011 ethyl palmitate, 0.027 ethyl oleate,

**Received:** November 16, 2010

**Accepted:** March 11, 2011

**Published:** March 23, 2011

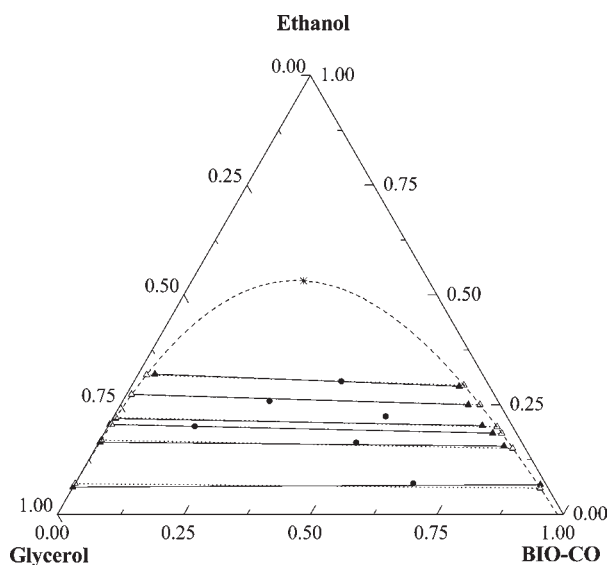


**Figure 1.** Experimental and calculated liquid–liquid equilibrium data for the BIO–CO + ethanol + glycerol system at  $T = 298.2$  K: ●, feed points; (▲, solid line), experimental tie lines; (△, dotted line), NRTL calculated tie lines; \*, NRTL calculated plait point; dashed line, NRTL calculated binodal curve.

0.049 ethyl linoleate, 0.004 ethyl linolenate, and 0.909 ethyl ricinoleate. The other chemical properties are described in Table 1.

**Procedure.** Experiments were carried out in glass equilibrium cells of approx. 45 mL equipped with an external jacket that maintains the interior cell temperature through circulation of water from a Tecnal TE-184 thermostatic bath, precise to  $\pm 0.1$  K.

For determining LLE data, mixtures with compositions within the immiscibility region were prepared directly inside the equilibrium cells. Each component was weighed using a Geraha AG200 analytical balance, precise to  $\pm 1 \cdot 10^{-6}$  kg. For ternary systems, the addition of each component was made following the order of volatility: biodiesel, glycerol, and ethanol; for quaternary, the order is biodiesel, glycerol, and NaOH + ethanol binary solution (NaOH needs first be solubilized in ethanol). The NaOH (feed) mass fraction used was  $0.0105 \pm 0.0004$  and  $0.0095 \pm 0.0002$  at (298.2 and 333.2) K, respectively.

The system was mixed at approximately 1200 rpm with a Fisatom 752 magnetic stirrer for 2 h to allow good contact between the phases, and was left to settle for 12 h until complete separation into two clean liquid phases. Preliminary experiments showed that the agitation and separation times were enough for the system to reach equilibrium.

Phase compositions in mass fraction were determined using the calibration curves reported as Supporting Information. Calibration curves were obtained by gas chromatography using an Agilent Technologies, Model 6850 CG System coupled with flame ionization detector (FID). The capillary column utilized was a SGE Forte BP-225 with 50%-cyanopropyl-phenyl 50%-dimethyl polysiloxane (25 m  $\times$  0.32 mm  $\times$  0.25  $\mu$ m). Nitrogen was used as a carrier gas at a flow rate of 1.0 mL/min. The column temperature was programmed from (308.15 to 458.15) K at the linear rate of 35 K/min. After, the temperature was programmed to reach 473.15 K in a linear rate of 5 K/min, keeping this for 2.5 min then heating at 10 K/min, to reach a final temperature of 503.15 K which was kept constant for 1.75 min.

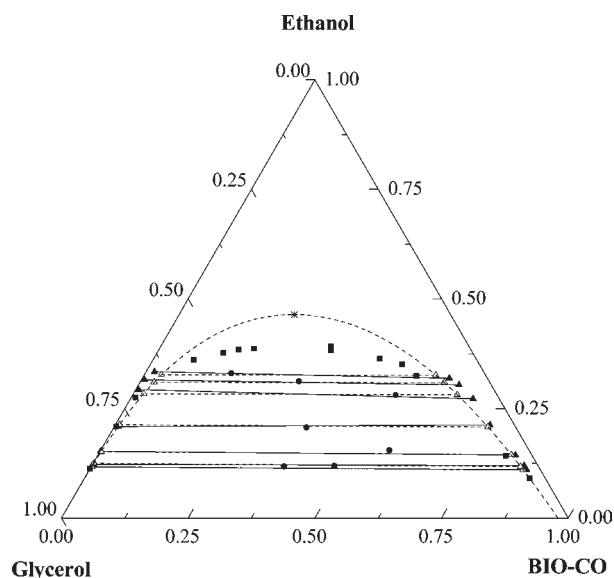


**Figure 2.** Experimental and calculated liquid–liquid equilibrium data for the BIO–CO + ethanol + glycerol system at  $T = 333.2$  K: ●, feed points; (▲, solid line), experimental tie lines; (△, dotted line), NRTL calculated tie lines; ■, cloud points of ref 16; \*, NRTL calculated plait point; dashed line, NRTL calculated binodal curve.

## ■ THERMODYNAMIC CORRELATIONS

The LLE calculation is basically defined by eq 1.

$$w_i^I \gamma_i^I = w_i^{II} \gamma_i^{II} \quad (1)$$

$\gamma_i$  and  $w_i$  represent the activity coefficient and mass fraction of component  $i$  present in both phases I and II. In this work, the well-known nonrandom two-liquid model (NRTL),<sup>17</sup> based on a local composition concept, was used to calculate the component activity coefficient in both phases. The model energy interaction and nonrandomness parameters were estimated by using a procedure similar to Stragevitch and D'Ávila.<sup>18</sup> This procedure is based on the modified Simplex method<sup>19</sup> and consists in the minimization of a concentration-based objective function,  $F$ ,<sup>20</sup> given by eq 2.

$$F = \sum_l^T \sum_k^D \sum_j^M \sum_i^{N-1} \{W_{ijkl} (w_{ijkl}^{\text{exp}} - w_{ijkl}^{\text{calc}})^2\} \quad (2)$$

$N$  is the number of components,  $j$  represents each tie line in a total of  $M$  tie lines,  $k$  represents each phase in a total of  $D$  phases,  $l$  represents each temperature in a total of  $T$  temperatures, exp and calc represent experimental and calculated data respectively, and  $W_{ijk}$  is the weight associated with component  $i$  in tie line  $j$  at phase  $k$  and temperature  $l$ . In this work,  $W_{ijk} = 1$  was used, which, according to Sørensen et al.,<sup>20</sup> neglects large relative errors between experimental and calculated compositions in small concentrations. Calculated compositions can be compared with the experimental ones through the percent root-mean-square (rms) deviation,  $\delta x$ , given by eq 3.

$$\delta x = 100 \sqrt{\frac{\sum_k^D \sum_j^M \sum_i^N (w_{ijk}^{\text{exp}} - w_{ijk}^{\text{calc}})^2}{2MN}} \quad (3)$$

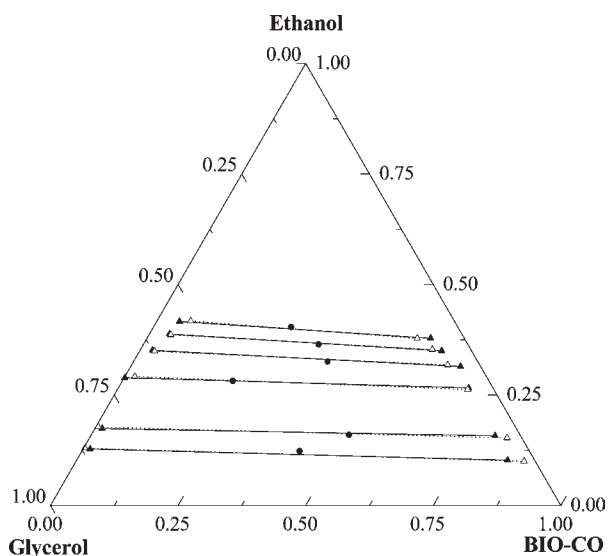


**Figure 3.** Experimental and calculated liquid–liquid equilibrium data for the BIO–CO + ethanol + glycerol system at  $T = 298.2$  K with 0.01 feed mass fraction of NaOH catalyst: ●, feed points; ▲, solid line), experimental tie lines; (△, dotted line), NRTL calculated tie lines.

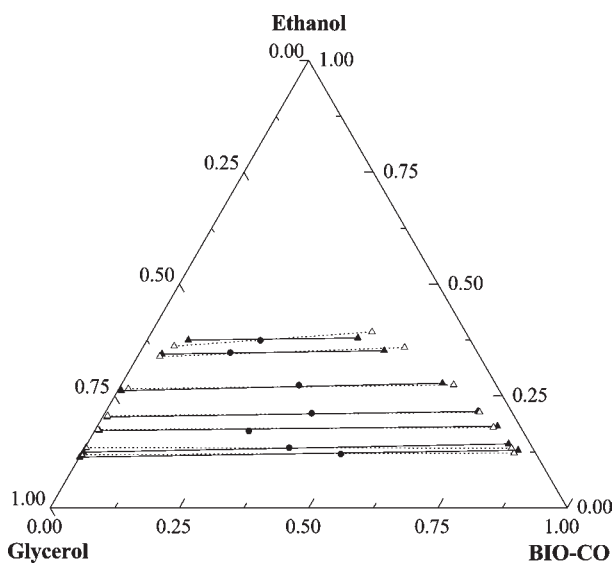


**Figure 4.** Experimental and calculated liquid–liquid equilibrium data for the BIO–CO + ethanol + glycerol system at  $T = 333.2$  K with 0.01 feed mass fraction of NaOH catalyst: ●, feed points; ▲, solid line), experimental tie lines; (△, dotted line), NRTL calculated tie lines.

## RESULTS AND DISCUSSION

**Liquid–Liquid Equilibrium Data.** LLE data obtained for ternary BIO–CO (1) + ethanol (2) + glycerol (3) and quaternary BIO–CO (1) + ethanol (2) + glycerol (3) + NaOH (4) at  $T = (298.2 \text{ and } 333.2)$  K and atmospheric pressure ( $\approx 95$  kPa) are shown in Figures 1–4 and reported in Tables 2 and 3. Uncertainties in mass fraction of each component were calculated to be less than  $10^{-4}$ . In Figures 3 and 4 the LLE data for quaternary systems are represented as pseudo ternary systems by inserting the NaOH composition into each component mass fraction using eq 4.

**Table 2.** Liquid–Liquid Equilibrium Data in Mass Fraction ( $w$ ) for BIO–CO (1) + Ethanol (2) + Glycerol (3)<sup>a</sup> at (298.2 and 333.2) K

$T$ K	feed		liquid–liquid equilibrium				$K^b$	$S^c$
			biodiesel-rich phase		glycerol-rich phase			
	$w_1$	$w_2$	$w_1$	$w_2$	$w_1$	$w_2$		
298.2	0.6685	0.0704	0.9213	0.0674	0.0000	0.0620	1.09	90.24
	0.5093	0.1634	0.8050	0.1559	0.0022	0.1646	0.95	20.18
	0.1716	0.2009	0.7678	0.1855	0.0013	0.2050	0.90	15.38
	0.5376	0.2230	0.7385	0.2025	0.0051	0.2184	0.93	12.20
	0.2904	0.2582	0.6872	0.2498	0.0100	0.2734	0.91	10.39
	0.4101	0.3032	0.6483	0.2922	0.0329	0.3200	0.91	9.93
333.2	0.3803	0.1181	0.8628	0.1104	0.0007	0.1166	0.95	31.19
	0.4789	0.1192	0.8530	0.1197	0.0022	0.1228	0.97	31.24
	0.5700	0.1543	0.8238	0.1439	0.0014	0.1521	0.95	24.79
	0.3801	0.2066	0.7396	0.2123	0.0084	0.2090	1.02	16.53
	0.5190	0.2806	0.6764	0.2721	0.0058	0.2930	0.93	12.64
	0.3117	0.3110	0.6329	0.3036	0.0064	0.3155	0.96	10.28
	0.1705	0.3302	0.6062	0.3191	0.0165	0.3340	0.96	8.31

<sup>a</sup>  $w_3 = 1 - w_1 - w_2$ . <sup>b</sup> Solute distribution coefficient, given by eq 5; <sup>c</sup> Biodiesel selectivity, given by eq 6.

$$w'_i = \frac{w_i}{1 - w_4} \quad (4)$$

In eq 4,  $i$  refers to components 1, 2, and 3,  $w'_i$  is the pseudo ternary system mass fraction, and  $w_i$  is the quaternary system mass fraction.

The study of the ethanol phase distribution was made from the solute distribution coefficient ( $K$ ) and the biodiesel selectivity ( $S$ ) given by eqs 5 and 6, respectively.

$$K = \frac{w_2^{\text{bio}}}{w_2^{\text{gly}}} \quad (5)$$

$$S = \frac{\frac{w_2^{\text{bio}}}{w_2^{\text{gly}}}}{\frac{w_3^{\text{bio}}}{w_3^{\text{gly}}}} \quad (6)$$

The superscripts bio and gly refer to the biodiesel-rich phase and glycerol-rich phase, respectively.

Ethanol distribution between the biodiesel-rich phase and glycerol-rich phase in the ternary system studied (without influence of NaOH) is not influenced by a temperature increase of 35 K; in the quaternary, the increase of 35 K in temperature gives a small enhancement in  $K$  values. At  $T = 298.2$  K, the 0.01 mass fraction of NaOH added to the ternary system does not affect the ethanol distribution, but at  $T = 333.2$  K, the presence of NaOH gives a small increase in ethanol partition. This behavior can be explained by an increase of ethanol solubility in the biodiesel-rich phase due to the presence of NaOH. So, for all systems studied, the only

**Table 3.** Liquid–Liquid Equilibrium Data in Mass Fraction ( $w$ ) for BIO–CO (1) + Ethanol (2) + Glycerol (3) + NaOH (4)<sup>a</sup> at (298.2 and 333.2) K

T	feed		liquid–liquid equilibrium data								
			biodiesel-rich phase			glycerol-rich phase			$K^b$	$S^c$	
	$w_1$	$w_2$	$w_3$	$w_1$	$w_2$	$w_3$	$w_1$	$w_2$			$w_3$
298.2	0.4222	0.1217	0.4451	0.8432	0.1025	0.0525	0.0138	0.1248	0.8386	0.82	13.12
	0.4997	0.1579	0.3314	0.7913	0.1571	0.0498	0.0144	0.1708	0.7973	0.92	14.73
	0.2145	0.2788	0.4963	0.6803	0.2635	0.0472	0.0009	0.2851	0.6997	0.92	13.70
	0.3765	0.3221	0.2909	0.6432	0.3126	0.0389	0.024	0.3477	0.6183	0.90	14.29
	0.3396	0.3612	0.2889	0.5894	0.3489	0.058	0.0389	0.3829	0.5656	0.91	8.89
	0.2672	0.3998	0.3226	0.5509	0.3749	0.065	0.0441	0.4093	0.5298	0.92	7.47
333.2	0.4975	0.1193	0.3735	0.8406	0.1284	0.0306	0.0008	0.1113	0.8717	1.15	32.86
	0.3917	0.1329	0.4659	0.8150	0.1426	0.0422	0.0023	0.1233	0.8648	1.16	23.70
	0.2962	0.1701	0.5243	0.7731	0.1820	0.0440	0.0089	0.1705	0.8099	1.07	19.65
	0.3964	0.2096	0.3847	0.7190	0.2154	0.0648	0.0083	0.2011	0.7799	1.07	12.89
	0.3412	0.2716	0.3775	0.6186	0.2777	0.1020	0.0067	0.2600	0.7259	1.07	7.60
	0.1736	0.3440	0.4732	0.4702	0.3509	0.1783	0.0441	0.3389	0.6030	1.04	3.20
	0.2177	0.3705	0.4021	0.4039	0.3777	0.2138	0.0785	0.3687	0.5357	1.02	2.57

<sup>a</sup>  $w_4 = 1 - w_1 - w_2 - w_3$ ; <sup>a</sup>  $w_3 = 1 - w_1 - w_2$ ; <sup>b</sup> Solute distribution coefficient, given by eq 5; <sup>c</sup> Biodiesel selectivity, given by eq 6.

**Table 4.** Hand<sup>a</sup> and Othmer-Tobias<sup>b</sup> Equation Coefficients ( $a$ ,  $b$ ) and Linear Coefficients of Determination ( $R^2$ )<sup>c</sup> and Standard Deviations ( $\sigma$ ) for Systems Studied in This Work

T	Hand				Othmer-Tobias			
	$a_H$	$b_H$	$R^2$	$\sigma_H$	$a_{OT}$	$b_{OT}$	$R^2$	$\sigma_{OT}$
BIO–CO (1) + Ethanol (2) + Glycerol (3)								
298.2	0.9080	-0.0684	0.9990	0.0097	0.8995	0.0066	0.9938	0.0251
333.2	1.0246	0.016	0.9959	0.018	0.9947	0.0758	0.9961	0.0174
BIO–CO (1) + Ethanol (2) + Glycerol (3) + NaOH (4)								
298.2	1.0156	-0.047	0.9939	0.0256	0.9274	-0.0391	0.9864	0.0326
333.2	1.0806	0.1351	0.9956	0.0220	1.1599	0.2493	0.9915	0.0348

<sup>a</sup> See eq 7. <sup>b</sup> See eq 8. <sup>c</sup> mass fraction range of validity: from the lower to the upper tie line composition for each temperature.

systems which presents  $K > 1$  is the BIO–CO + ethanol + glycerol + NaOH at  $T = 333.2$  K.

The selectivity of biodiesel gives its preference to solubilize ethanol (a solute) or glycerol (a diluent). Here all systems presented  $S$  values between 2 and 90. Also, as shown in Tables 2 and 3, a decrease in ethanol mass fraction in the glycerol-rich phase gives an increase in selectivity of biodiesel for ethanol. This probably occurs because the presence of ethanol in the glycerol-rich phase enhances the solubility of this phase in the biodiesel-rich phase, which solubilizes an amount of glycerol together with ethanol, diminishing the  $S$  value.

The quality of the LLE data was pointed out by two factors: (a) agreement of tie lines with the feed composition, indicating low experimental error by loss of mass or analysis, and (b) testing the LLE data with Hand<sup>21</sup> and Othmer-Tobias<sup>22</sup> correlations (eqs 7 and 8, respectively).

$$\log_{10} \left( \frac{w_2^{\text{bio}}}{w_1^{\text{bio}}} \right) = a_H \log_{10} \left( \frac{w_2^{\text{gly}}}{w_3^{\text{gly}}} \right) + b_H \quad (7)$$

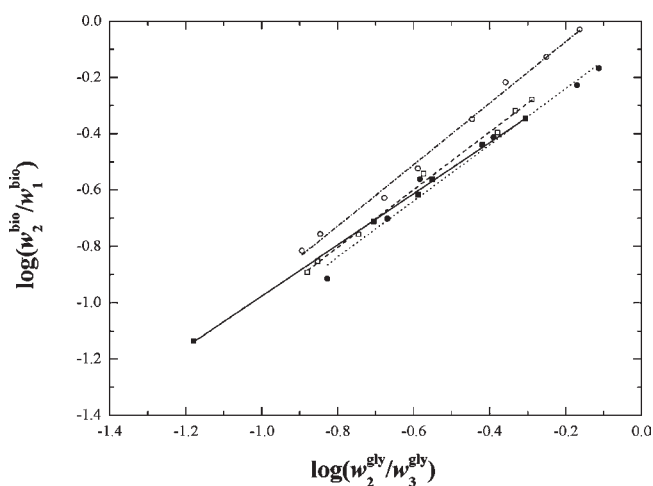


**Figure 5.** Hand plot for LLE data determined in this work. (■, solid line), BIO–CO + ethanol + glycerol at 298.2 K; (□, dashed line), BIO–CO + ethanol + glycerol at 333.2 K; (●, dotted line), BIO–CO + ethanol + glycerol + NaOH at 298.2 K; (○, dash dot line), BIO–CO + ethanol + glycerol + NaOH at 333.2 K.

$$\log_{10} \left( \frac{1 - w_1^{\text{bio}}}{w_1^{\text{bio}}} \right) = a_{OT} \log_{10} \left( \frac{1 - w_3^{\text{gly}}}{w_3^{\text{gly}}} \right) + b_{OT} \quad (8)$$

$a$  are the angular coefficients and  $b$  are the linear coefficients. The standard deviations for Hand ( $\sigma_H$ ) and Othmer-Tobias ( $\sigma_{OT}$ ) were calculated with eq 9.

$$\sigma_H = \sigma_{OT} = \sqrt{\sum_i^d \frac{(L_{\text{exp}} - L_{\text{calc}})_i^2}{d - p}} \quad (9)$$

$L$  refers to the left-hand side of each correlation (Hand and/or Othmer-Tobias),  $d$  represents the number of data points

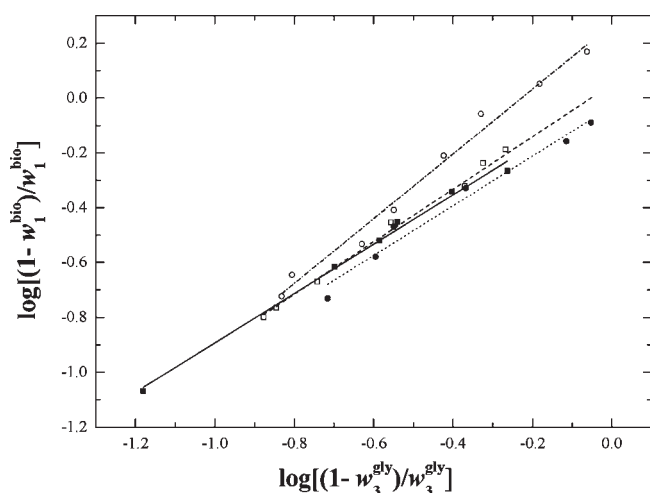


**Figure 6.** Othmer-Tobias plot for LLE data determined in this work. (■, solid line), BIO-CO + ethanol + glycerol at 298.2 K; (□, dashed line), BIO-CO + ethanol + glycerol at 333.2 K; (●, dotted line), BIO-CO + ethanol + glycerol + NaOH at 298.2 K; (○, dash dot line), BIO-CO + ethanol + glycerol + NaOH at 333.2 K.

**Table 5.** Estimated NRTL Parameters ( $A$ ,  $B$ ) and Root-Mean-Square Deviations ( $\delta x$ )<sup>a</sup>

$i$	$j$	$A_{ij}$	$A_{ji}$	$B_{ij}$	
				K	K
BIO-CO (1), Ethanol (2), Glycerol (3), NaOH (4), $\delta x = 1.299\%$					
1	2	-907.52	1192.30	3.39	-3.52
1	3	1476.90	36.96	-1.83	8.89
1	4	766.52	-789.25	6.67	0.03
2	3	188.40	7.31	-0.03	-0.03
2	4	-89.21	-1291.20	-8.74	-0.04
3	4	-1063.80	-1022.10	0.26	-0.08

<sup>a</sup>  $\alpha_{ij} = \alpha_{ji}$  was kept constant and equal to 0.2.

(tie lines), and  $p$  is the number of parameters in the Hand and Othmer-Tobias equations ( $p = 2$ ). The data quality is shown by a  $R^2 > 0.99$ ,  $\sigma_H < 0.0256$ , and  $\sigma_{OT} < 0.0348$  achieved for all systems, as presented in Table 4 and Figures 5 and 6.

**NRTL Parameters.** The NRTL parameters estimated here are shown in Table 5, and the calculated tie lines are shown in Figures 1–4. The model correlates well the experimental data, presenting percent root-mean-square deviation smaller than 1.3% for the ternary and quaternary systems studied here, respectively.

## CONCLUSION

Ternary and quaternary LLE data for castor oil biodiesel (BIO-CO) + ethanol + glycerol and quaternary LLE data for biodiesel (BIO-CO) + ethanol + glycerol + NaOH (0.01 mass fraction) systems at  $T = (298.2 \text{ and } 333.2) \text{ K}$  and atmospheric pressure ( $\approx 95 \text{ kPa}$ ) were obtained. The system which presents higher values of ethanol distribution and selectivity is biodiesel (BIO-CO) + ethanol + glycerol + NaOH at  $T = 333.2 \text{ K}$ . The NRTL model correlates well the experimental data, presenting a root-mean-square deviations  $< 1.3 \%$  for all systems. The quality

of experimental tie lines is assured by the Hand and Othmer-Tobias correlations ( $R^2 > 0.98$ ) for all systems.

## ASSOCIATED CONTENT

**Supporting Information.** Table S1: Components calibration curves of mass fraction ( $w$ ) versus peak area ( $A$ ). This material is available free of charge via the Internet at <http://pubs.acs.org>.

## AUTHOR INFORMATION

### Corresponding Author

\*Tel.: +55 19 3521 3957. E-mail: [wolf@feq.unicamp.br](mailto:wolf@feq.unicamp.br).  
†E-mail: [machadoparana@yahoo.com.br](mailto:machadoparana@yahoo.com.br).

### Funding Sources

The financial support from the Brazilian agency FAPESP is gratefully acknowledged.

## REFERENCES

- (1) Conceição, M. M.; Fernandes, V. J., Jr.; Araújo, A. S.; Farias, M. F.; Santos, I. M. G.; Souza, A. G. Thermal and Oxidative Degradation of Castor Oil Biodiesel. *Energy Fuel* **2007**, *21*, 1522–1527.
- (2) Fukuda, H.; Kondo, A.; Noda, H. J. Biodiesel fuel production by transesterification of oils. *J. Biosci. Bioeng.* **2001**, *92*, 405–16.
- (3) Berchmans, H. J.; Hirata, S. Biodiesel Production from Crude *Jatropha curcas* L. Seed Oil with a High Content of Free Fatty Acids. *Bioresour. Technol.* **2008**, *99*, 1716–1721.
- (4) Zhang, S.; Maréchal, F.; Gassner, M.; Périn-Levasseur, Z.; Qi, W.; Ren, Z.; Yan, Y.; Favrat, D. *Energy Fuel* **2009**, *23*, 1759–1765.
- (5) Komers, K.; Tichý, J.; Skopal, F. Ternäres Phasendiagramm Biodiesel-Methanol-Glycerin. *J. Prakt. Chem.* **1995**, *337*, 328–331.
- (6) Zhou, H.; Lu, H.; Liang, B. Solubility of Multicomponent Systems in the Biodiesel Production by Transesterification of *Jatropha curcas* L. Oil with Methanol. *J. Chem. Eng. Data* **2006**, *51*, 1130–1135.
- (7) Negi, D. S.; Sobotka, F.; Kimmel, T.; Wozny, G.; Schomäcker, R. Liquid-Liquid Phase Equilibrium in Glycerol-Methanol-Methyl Oleate and Glycerol-Monoolein-Methyl Oleate Ternary Systems. *Ind. Eng. Chem. Res.* **2006**, *45*, 3693–3696.
- (8) Andreatta, A. E.; Casás, L. M.; Hegel, P.; Bottini, S. B.; Brignole, E. A. Phase Equilibria in Ternary Mixtures of Methyl Oleate, Glycerol, and Methanol. *Ind. Eng. Chem. Res.* **2008**, *47*, 5157–5164.
- (9) Liu, X.; Piao, X.; Wang, Y.; Zhu, S. Liquid-Liquid Equilibrium for Systems of (Fatty Acid Ethyl Esters + Ethanol + Soybean Oil and Fatty Acid Ethyl Esters + Ethanol + Glycerol). *J. Chem. Eng. Data* **2008**, *53*, 359–362.
- (10) Tizvar, R.; McLean, D. D.; Kates, M.; Dubé, M. A. Optimal Separation of Glycerol and Methyl Oleate via Liquid-Liquid Extraction. *J. Chem. Eng. Data* **2009**, *54*, 1541–1550.
- (11) França, B. B.; Pinto, F. M.; Pessoa, F. L. P.; Uller, A. M. C. Liquid-Liquid Equilibria for Castor Oil Biodiesel + Glycerol + Alcohol. *J. Chem. Eng. Data* **2009**, *54*, 2359–2364.
- (12) Barreau, A.; Brunella, I.; Hemptinne, J.-C.; Coupard, V.; Canet, X.; Rivollet, F. Measurements of Liquid-Liquid Equilibria for a Methanol + Glycerol + Methyl Oleate System and Prediction Using Group Contribution Statistical Associating Fluid Theory. *Ind. Eng. Chem. Res.* **2010**, *49*, 5800–5807.
- (13) Follegatti-Romero, L. A.; Lanza, M.; Batista, F. R. M.; Batista, E. A. C.; Oliveira, M. B.; Coutinho, J. A. P.; Meirelles, A. J. A. Liquid-Liquid Equilibrium for Ternary Systems Containing Ethyl Esters, Anhydrous Ethanol and Water at 298.15, 313.15, and 333.15 K. *J. Chem. Eng. Data* **2010**, doi: 10.1021/ie101611j.
- (14) Lanza, M.; Borges Neto, W.; Batista, E.; Poppi, R. J.; Meirelles, A. J. A. Liquid-Liquid Equilibrium Data for Reactional Systems of Ethanolysis at 298.3 K. *J. Chem. Eng. Data* **2008**, *53*, 5–15.

(15) Felice, R. D.; Faveri, R. D.; Andreis, P. D.; Ottonello, P. Component Distribution between Light and Heavy Phases in Biodiesel Processes. *Ind. Eng. Chem. Res.* **2008**, *47*, 7862–7867.

(16) Ardila, Y. C.; Pinto, G. M. F.; Machado, A. B.; Wolf Maciel, M. R. Experimental Determination of Binodal Curves and Study of the Temperature in Systems Involved in the Production of Biodiesel with Ethanol. *J. Chem. Eng. Data* **2010**, *55*, 4592–4596.

(17) Renon, H.; Prausnitz, J. M. Local Compositions in Thermodynamic Excess Functions for Liquid Mixtures. *AIChE J.* **1968**, *14*, 135–144.

(18) Stragevitch, L.; d'Avila, S. G. Application of a Generalized Maximum Likelihood Method in the Reduction of Multicomponent Liquid-Liquid Equilibrium Data. *Braz. J. Chem. Eng.* **1997**, *14*, 41–52.

(19) Nelder, J. A.; Mead, R. A Simplex Method for Function Minimization. *Computer J.* **1965**, *7*, 308–313.

(20) Sørensen, J. M.; Magnussen, T.; Rasmussen, P.; Fredenslund, A. Liquid-liquid Equilibrium Data: Their Retrieval, Correlation and Prediction. Part II: Correlation. *Fluid Phase Equilib.* **1979**, *3*, 47–82.

(21) Hand, D. B. Dimeric Distribution. *J. Phys. Chem.* **1930**, *34*, 1961–2000.

(22) Othmer, D. F.; Tobias, P. E. Tie-line Correlation. *Ind. Eng. Chem.* **1942**, *34*, 693–696.